Electronic Supplementary Material (ESI) for ChemComm.

Supporting Information

Reactivity of mono- and divalent aluminium compounds towards group 15 nanoparticles

Adrian Hauser, Luca Muenzfeld and Peter W. Roesky*

General Methods:

All manipulations of air-sensitive materials were performed under rigorous exclusion of oxygen and moisture in flame-dried Schlenk-type glassware either on a dual manifold Schlenk line, interfaced to a high vacuum (10-3 torr) pump, or in an argon-filled MBraun glove box. Hydrocarbon solvents were pre-dried using an MBraun solvent purification system (SPS-800), degassed and stored in vacuo over $LiAlH_4$. Tetrahydrofuran was additionally distilled under nitrogen over potassium before storage in vacuo over $LiAlH_4$. THF was dried over K and degassed by freeze-pump-thaw cycles. Elemental analyses were carried out with an Elementar Vario MICRO Cube. NMR spectra were recorded on Bruker spectrometers (Avance III 300 MHz, Avance 400 MHz, or Avance III 400 MHz). Chemical shifts are referenced internally using signals of the residual protio solvent (^{1}H) or the solvent ($^{13}C\{^{1}H\}$) and are reported relative to tetramethylsilane (^{1}H, $^{13}C\{^{1}H\}$). All NMR spectra were measured at 298 K. Raman spectra were recorded in the region 4000-20 cm^{-1} on a Bruker MultiRam spectrometer equipped with a Nd:YAG laser (λ = 1064 nm) and a germanium detector at a resolution of 2 cm^{-1}. The powdered crystalline sample materials were flame sealed in a glass tube. The laser energy was adjusted to values between 20 and 200 mW depending on the FID amplitude and laser focusing. In terms of their intensity, the signals were classified into different categories (vs = very strong, s = strong, m = medium, w = weak).

Note: To ensure the best possible purity and reliability of all compounds, only crystalline material was isolated. Hence all yields and analytics refer to isolated crystalline samples, whereas yields are generally lower compared to bulk samples.

Sb^{0}_{nano}, As^{0}_{nano} and $[AlCp^*]_4$ (Cp* = pentamethylcyclopentadienyl) were synthesized following literature procedures.[1, 2, 3]

***Caution**: Arsenic, Antimony and their derivatives are toxic.*

Synthesis of $[AlCp^*X]_2$ (X = Br, I)):

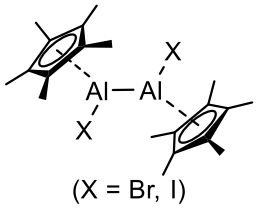

(X = Br, I)

The synthesis was carried out according to a modified procedure by *Braunschweig et al.* and *Arnold et al.*.[4, 5]

A solution of $[Cp^*AlI(\mu\text{-}X)]_2$ (X = Br, I) (2.45 mmol, 1.00 eq, (X = Br 1.58 g; X = I 2.04 g)) in toluene (20 mL) was added to Na/K alloy prepared from sodium (0.041 g, 1.78 mmol) and potassium (0.129 g, 3.30 mmol) in toluene (10 mL) and stirred for 16 h at room temperature. The yellow solution was filtrated and concentrated to 5 mL *in vacuo*. After storage at -10 °C yellow crystals formed. Separation of the crystals from the mother liquor yielded analytical pure compounds.

Yield: X = Br 580 mg (1.20 mmol, 49%); X = I 540 mg (0.934 mmol, 38%).

The NMR spectra are in agreement with literature.[4, 5]

(X = Br): **^{1}H NMR** (400.30 MHz, C_6D_6, 300 K) *δ*/ppm = 1.85 (s, 30 H, $C_5\underline{Me}_5$) ppm.

(X = I): **^{1}H NMR** (400.30 MHz, C_6D_6, 300 K) *δ*/ppm = 1.80 (s, 30 H, $C_5\underline{Me}_5$) ppm.

Synthesis of $[(Cp^*Al)_6As_4]$ (1) and $[(Cp^*Al)_6As_5Al]$ (2)

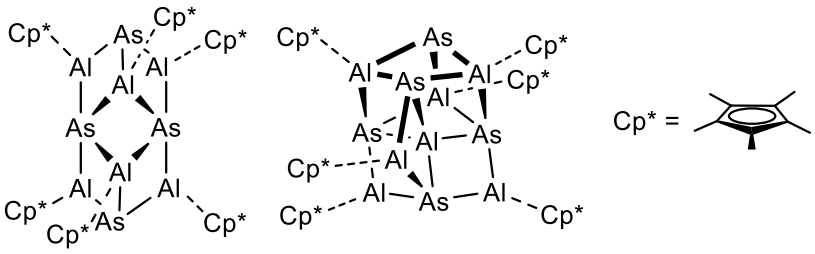

1 **2**

Toluene (15 ml) was condensed to a mixture of 200 mg $[AlCp^*]_4$ (0.308 mmol, 1.00 eq) and 92.0 mg As^0_{nano} (0.413 mmol, 4.00 eq). After sonification for 8 h the brownish suspension was stirred at 70 °C for 7 days. Separation of excess nanoparticles by filtration resulted in an orange/red solution. This solution was concentrated *in vacuo* until crystallization was imminent. Crystals suitable for X-ray diffraction of compound **1** could be obtained by recrystallization from hot toluene solution. Afterwards, suitable crystals for X-ray diffraction of compound **2** were obtained from hot benzene. Neither variation of stoichiometry, nor reaction conditions led to the sole formation of one of the compounds. However, further characterisation of compounds **1** and **2** could be achieved by manually separating sufficient crystals.

[(Cp*Al)$_6$As$_4$] (1) (yellow crystals):

^{1}H NMR (400.30 MHz, toluene-d_8, 300 K) δ = 2.05 (s, 90 H, C$_5$*Me$_5$*) ppm. **^{13}C{^{1}H} NMR** (100.67 MHz, toluene-d_8) δ = 115.9 (*C$_5$*Me$_5$), 11.7 (C$_5$*Me$_5$*) ppm.

Raman: $\tilde{\nu}$ [cm^{-1}] = 2968 (w), 2912 (w), 2861 (w), 2724 (w), 1462 (w), 1425 (w), 1385 (w), 1369 (w), 593 (m), 557 (w), 532 (w), 384 (w), 350 (w), 272 (w), 215 (w), 131 (w), 104 (m) 81 (vs).

[(Cp*Al)$_6$As$_5$Al] (2) (red crystals):

^{1}H NMR (400.30 MHz, toluene-d_8, 300 K) δ = 2.03 (s, 90 H, C$_5$*Me$_5$*) ppm. **^{13}C{^{1}H} NMR** Due to solubility problems no ^{13}C{^{1}H} NMR could be obtained.

Raman: $\tilde{\nu}$ [cm^{-1}] = 2910 (m), 2855 (w), 2721 (w), 1456 (w), 1424 (w), 1382 (w), 1030 (w), 1003 (w), 788 (w), 595 (w), 555 (w), 473 (w), 374 (w), 345 (w), 304 (w), 282 (w), 232 (w), 133 (s), 88 (vs), 69 (vs).

Synthesis of [(Cp*Al)$_3$Sb] (3)

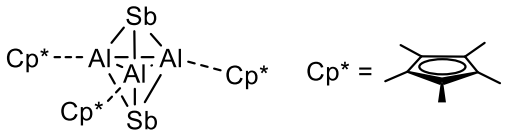

In a reaction flask 100 mg [AlCp*]$_4$ (0.154 mmol, 1.00 eq) was placed together with 75.0 mg of Sb$^0_{nano}$ (0.616 mmol, 4.00 eq). After condensation of toluene (15 ml) and sonification for 8 h, the mixture was heated to 130 °C and stirred for 7 days. Following filtration of excess nanoparticles, the orange solution was concentrated *in vacuo* until crystallization was imminent. Crystals suitable for X-ray diffraction could be obtained by recrystallization from hot toluene. NMR-spectra as well as the measured unit cell of the single crystals agree with literature data (see X-ray crystallographic studies).[6, 7]

Yield: 32.0 mg (0.044 mmol, 21%).

^{1}H NMR (400.30 MHz, C$_6$D$_6$, 300 K) δ = 2.08 (s, 45 H, C$_5$*Me$_5$*) ppm. **^{13}C{^{1}H} NMR** (100.67 MHz, C6D6) δ = 116.1 (*C$_5$*Me$_5$), 12.0 (C$_5$*Me$_5$*) ppm.

Synthesis of [(Cp*AlBr)$_3$As] (4)

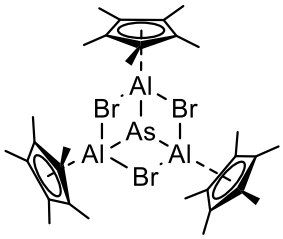

A mixture of 200 mg [Cp*AlBr]$_2$ (0.413 mmol, 1.00 eq) and 31.0 mg As$^0_{nano}$ (0.413 mmol, 1.00 eq) was suspended toluene (15 ml). The reaction mixture was alternately sonicated and stirred at 80 °C for 8 h each in the course of 4 days. Afterwards, the excess of As$^0_{nano}$ was removed by filtration and the yellow solution was concentrated *in vacuo* to approximately 3 ml. Yellow crystals of compound **4** were obtained after storage at -10 °C.

Yield: 113 mg (0.140 mmol, 51%).

^{1}H NMR (400.30 MHz, C_6D_6, 300 K) δ = 1.95 (s, 45 H, $C_5\underline{Me_5}$) ppm. **^{13}C{^{1}H} NMR** (100.67 MHz, C6D6) δ = 116.5 ($\underline{C_5}Me_5$), 11.7 ($C_5\underline{Me_5}$) ppm.

Raman: $\tilde{\nu}$ [cm^{-1}] = 2913 (m), 2859 (w), 1456 (w), 1423 (w), 1385 (w), 595 (w), 554 (w), 366 (w), 183 (s), 87 (s).

Anal. calcd. (%) for [$C_{30}H_{45}Al_3AsBr_3$]: (801.27 g/mol): C: 44.97, H: 5.66; **found** (%): C: 44.99, H: 5.478.

Synthesis of [(Cp*AlI)$_3$As] (5)

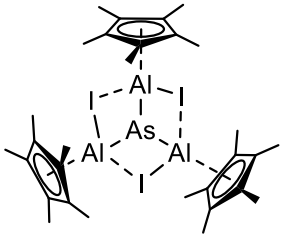

To a mixture of 200 mg [CpAlI]$_2$ (0.346 mmol, 1.00 eq) and 26.0 mg As$^0_{nano}$ (0.346 mmol, 1.00 eq) toluene (15 ml) was condensed. Reaction and crystallization were carried out as described for compound **4**.

Yield: 63.0 mg (0.067 mmol, 29%).

^{1}H NMR (400.30 MHz, C_6D_6, 300 K) δ = 1.91 (s, 45 H, $C_5\underline{Me_5}$) ppm. **^{13}C{^{1}H} NMR** (100.67 MHz, C6D6) δ = 117.2 ($\underline{C_5}Me_5$), 12.6 ($C_5\underline{Me_5}$) ppm.

Raman: $\tilde{\nu}$ [cm^{-1}] = 2911 (m), 2858 (w), 1459 (w), 1421 (w), 1384 (w), 595 (m), 554(w), 370 (w), 164 (m), 130 (s), 89 (s), 71 (vs).

Anal. calcd. (%) for [$C_{30}H_{45}Al_3AsI_3$]: (942.27 g/mol): C: 38.24, H: 4.81; **found** (%): C: 38.43, H: 4.785.

NMR Spectra of 1-5

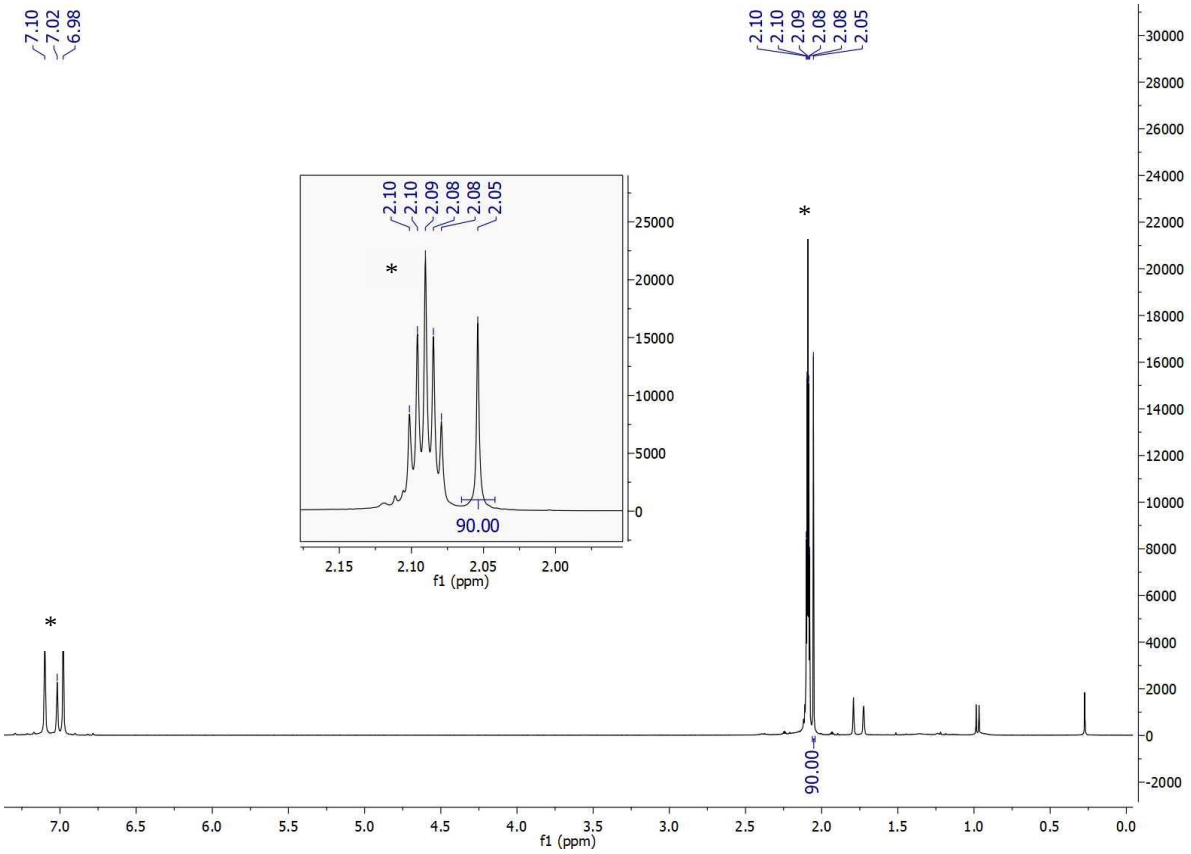

Figure S1: ^{1}H NMR of [(Cp*Al)$_6$As$_4$] (**1**) in toluene-d_8. *, residual protio solvent signal.

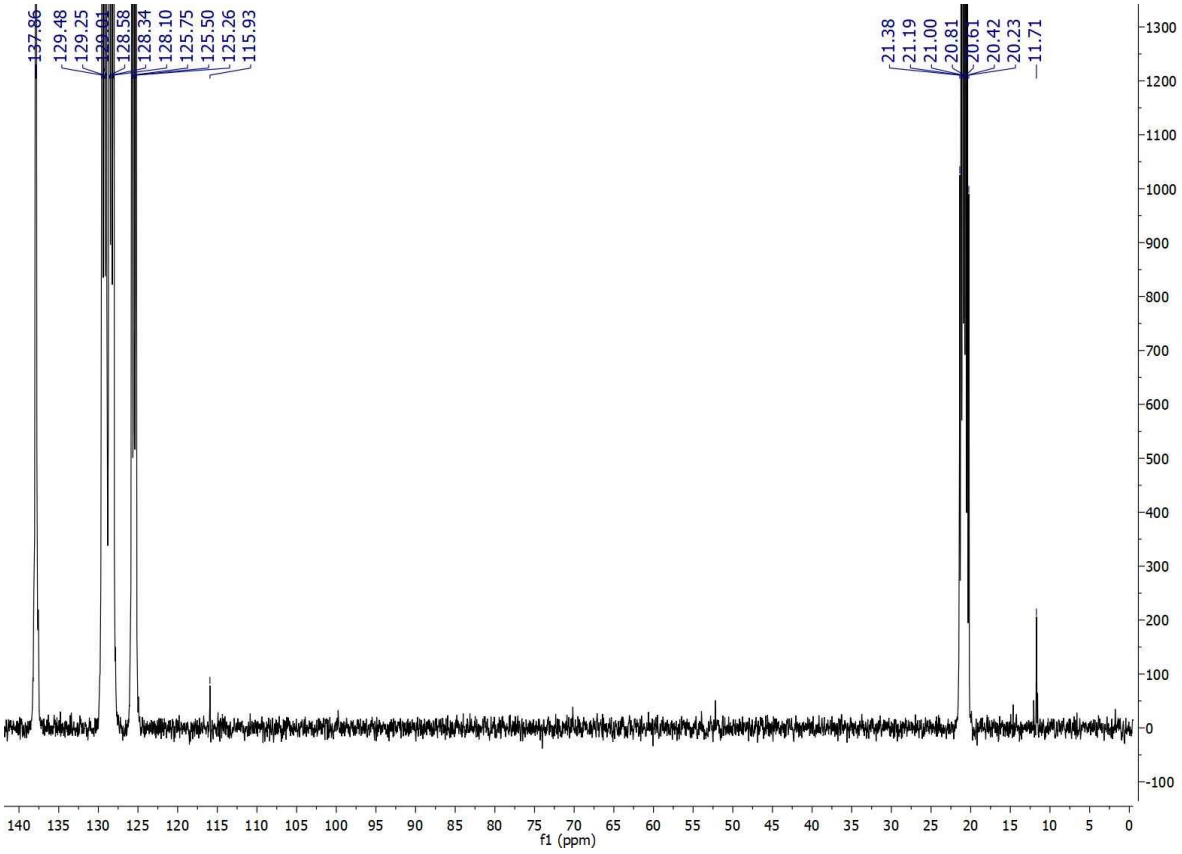

Figure S2: ^{13}C{^{1}H} NMR of [(Cp*Al)$_6$As$_4$] (**1**) in toluene-d_8.

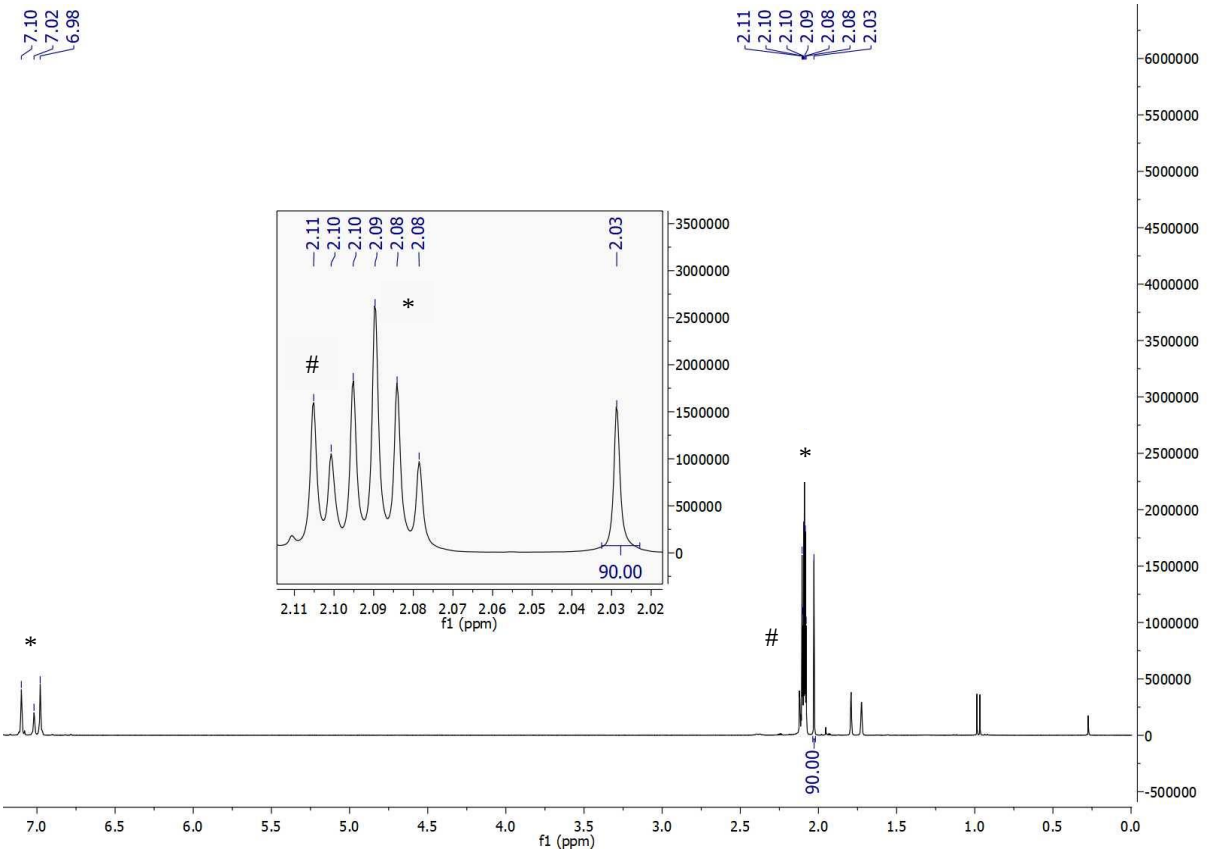

Figure S3: ^{1}H NMR of [(Cp*Al)$_6$As$_5$Al] (**2**) in toluene-*d*$_8$. *, residual protio solvent signal. #, residual toluene signal from mother liquor.

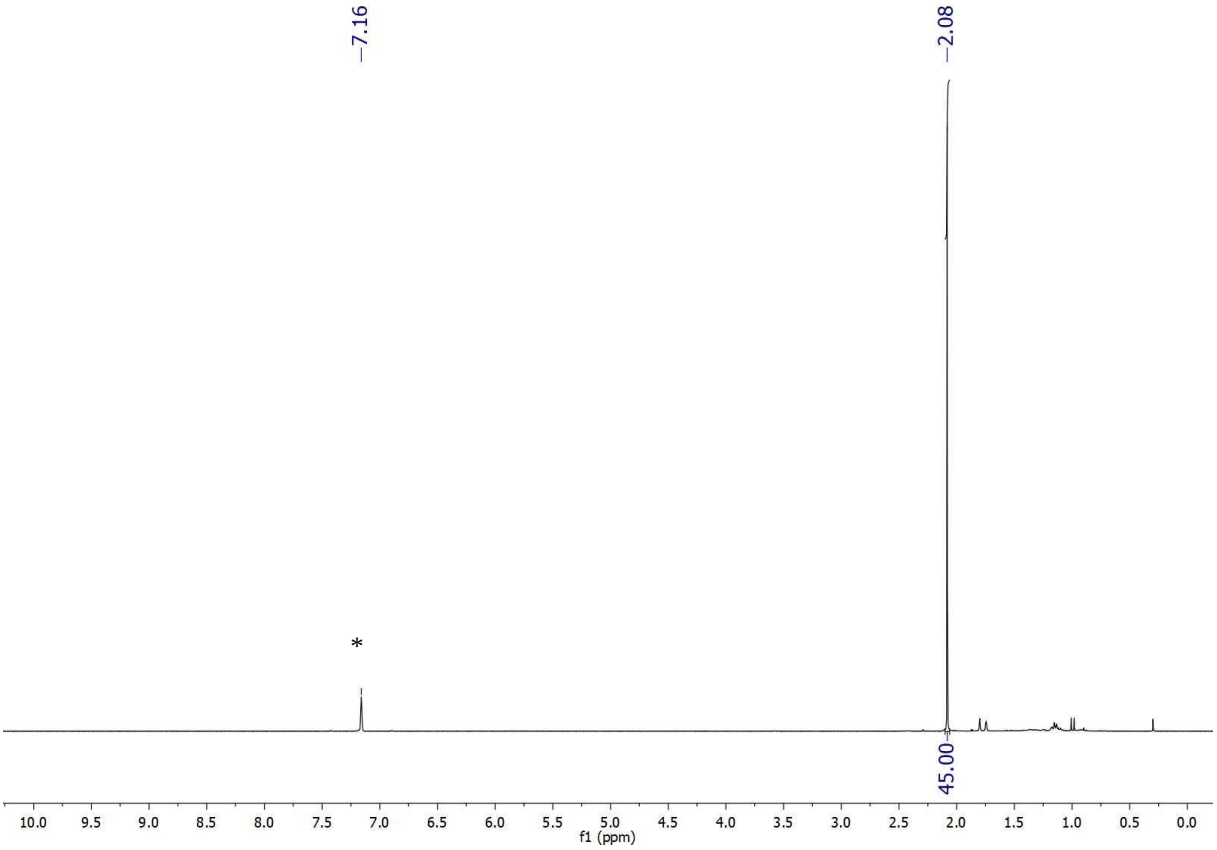

Figure S4: ^{1}H NMR of $[(Cp^*Al)_3Sb]$ (**3**) in C_6D_6. *, residual protio solvent signal.

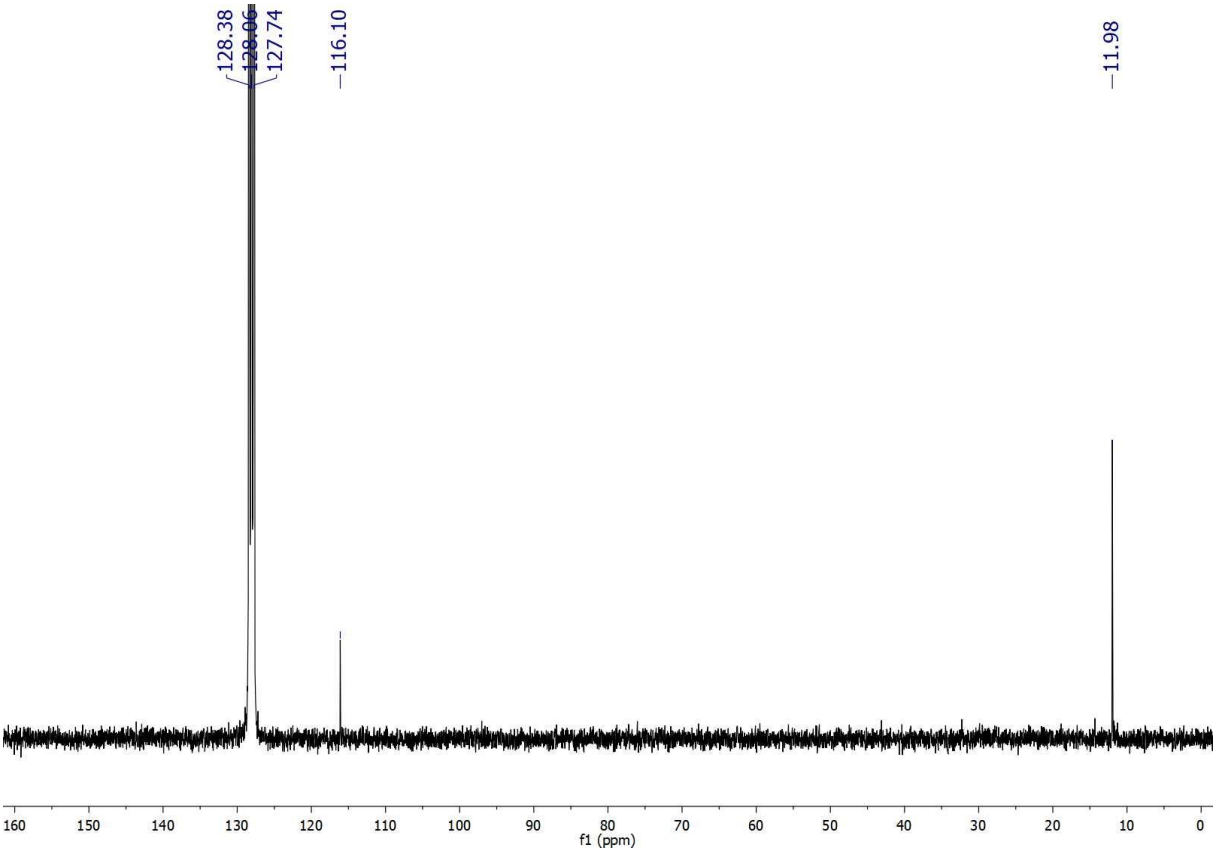

Figure S5: $^{13}C\{^{1}H\}$ NMR of $[(Cp^*Al)_3Sb]$ (**3**) in C_6D_6.

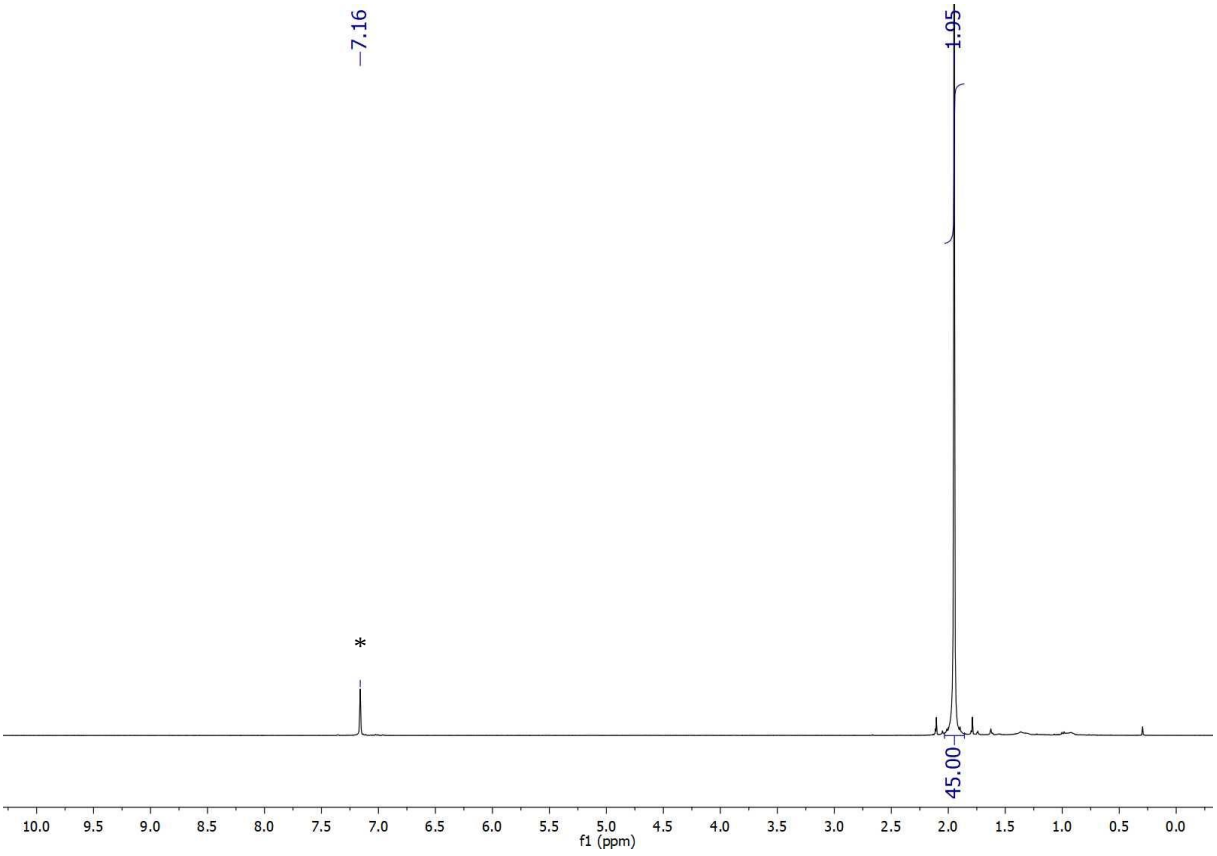

Figure S6: ^{1}H NMR of of $[(Cp^*AlBr)_3As]$ (**4**) in C_6D_6. *, residual protio solvent signal.

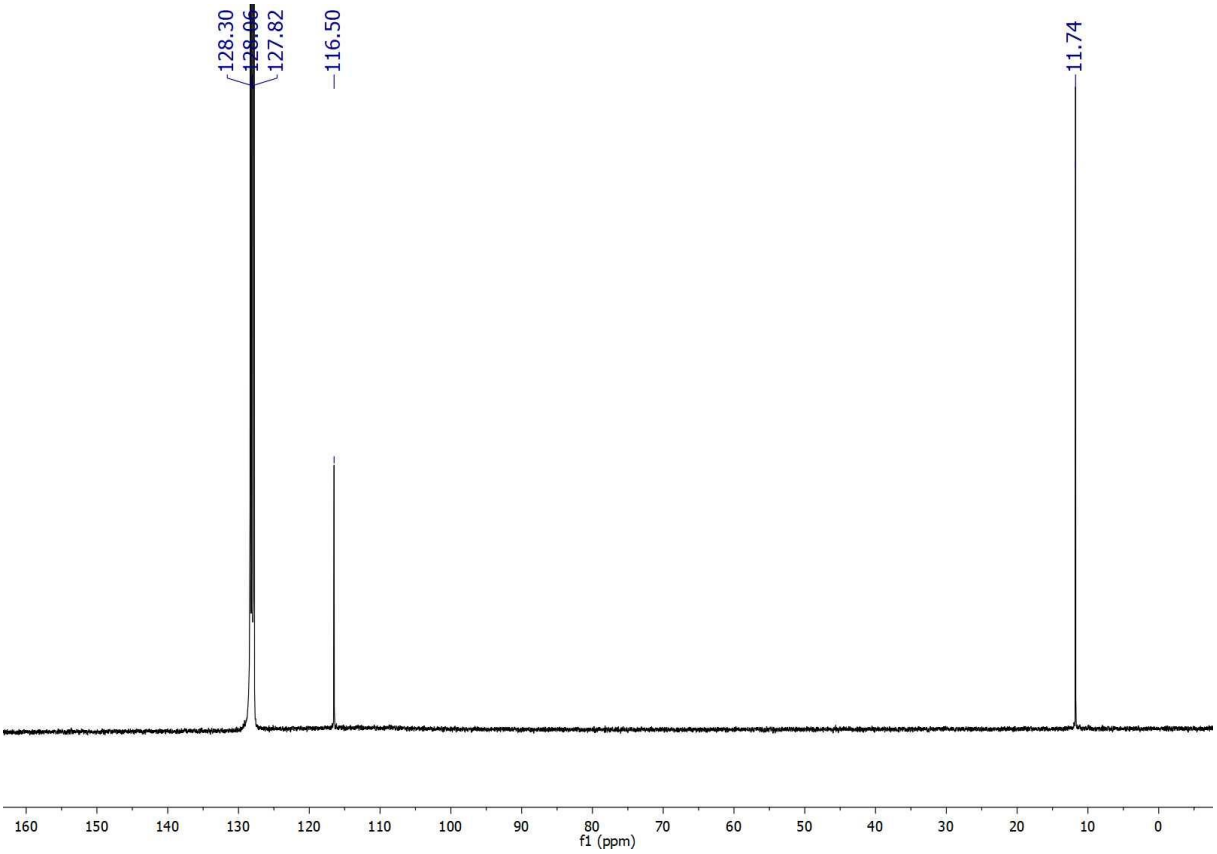

Figure S7: $^{13}C\{^{1}H\}$ NMR of $[(Cp^*AlBr)_3As]$ (**4**) in C_6D_6.

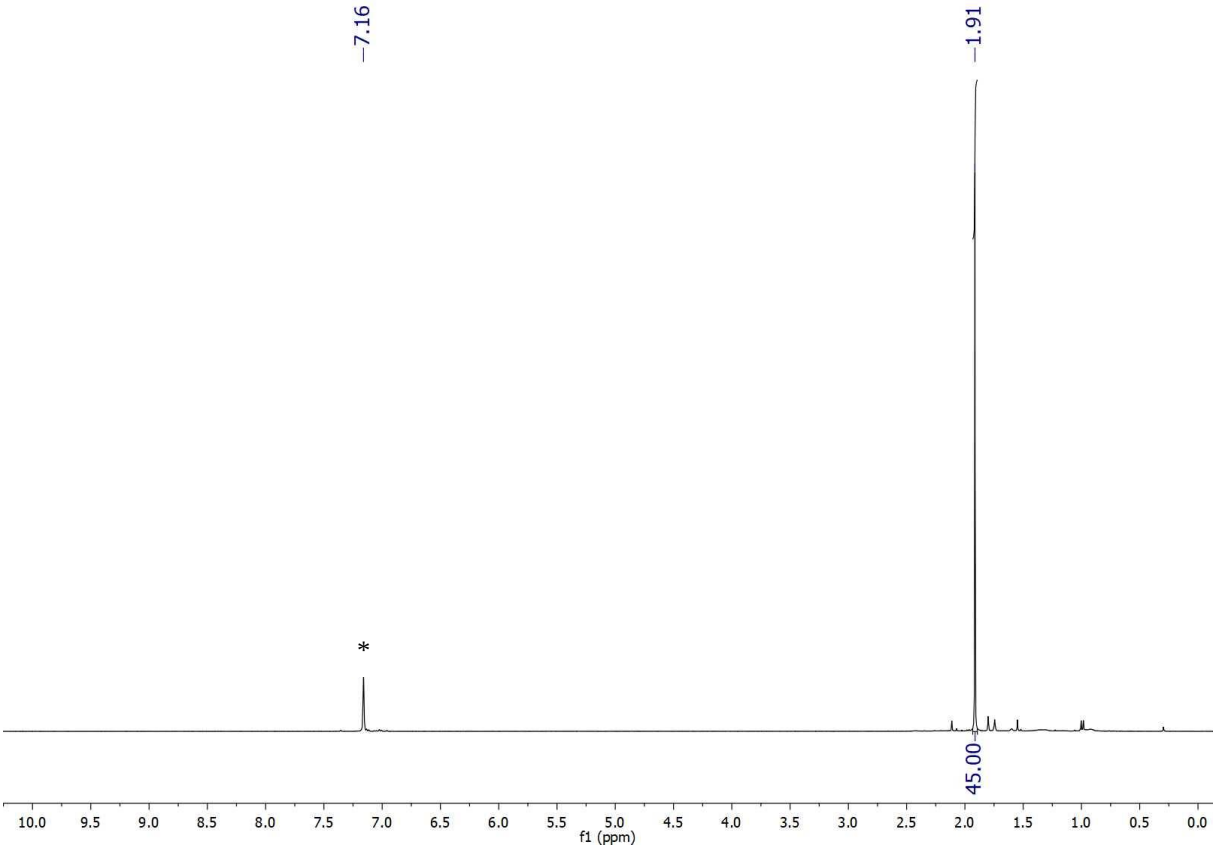

Figure S8: ^{1}H NMR of of $[(Cp^*Al)_3As]$ (**5**) in C_6D_6. *, residual protio solvent signal.

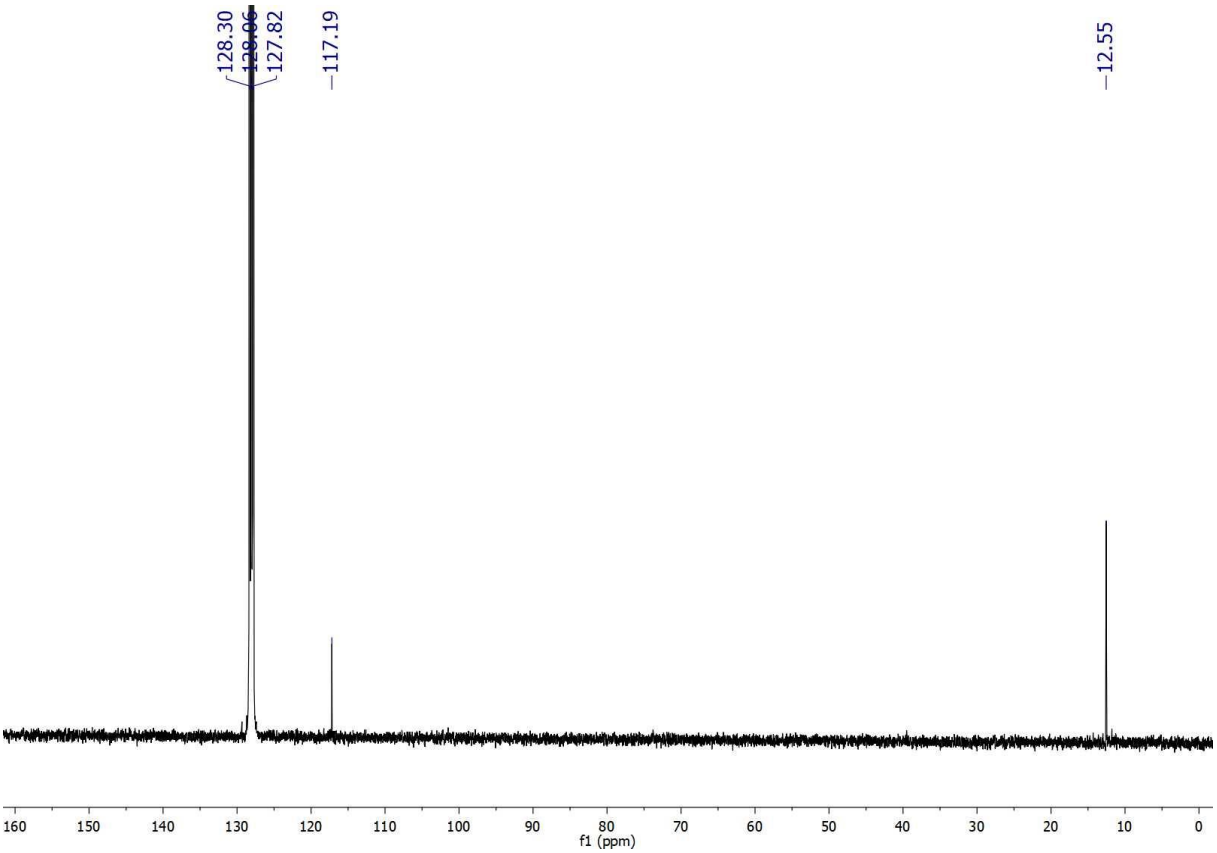

Figure S9: $^{13}C\{^{1}H\}$ NMR of $[(Cp^*Al)_3As]$ (**5**) in C_6D_6.

FT-Raman Spectra of 1,2,4 and 5

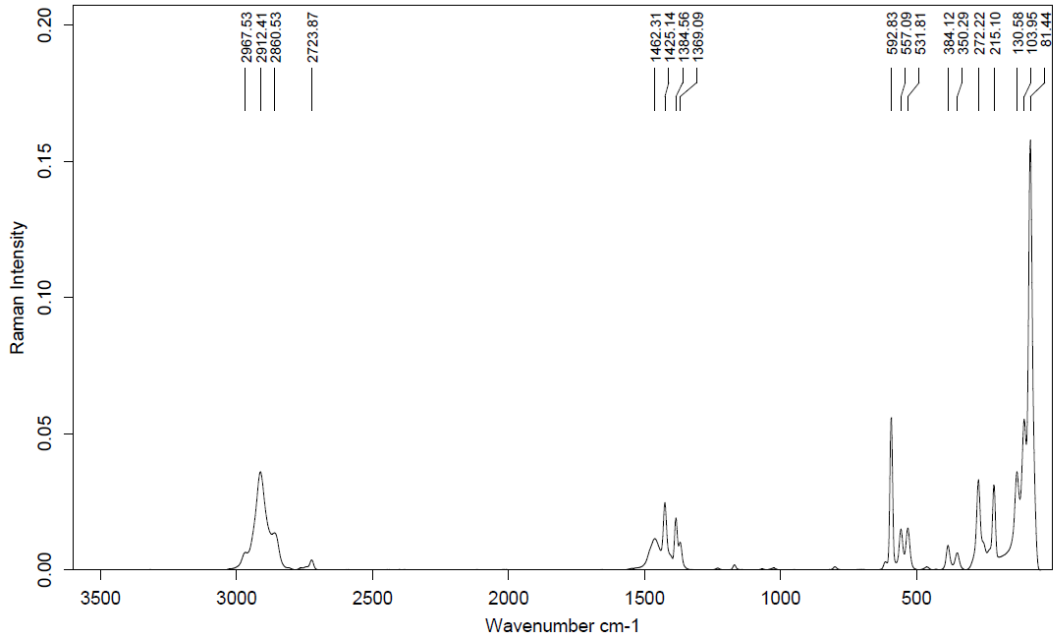

Figure S10: FT-Raman spectrum of $[(Cp^*Al)_6As_4]$ (**1**).

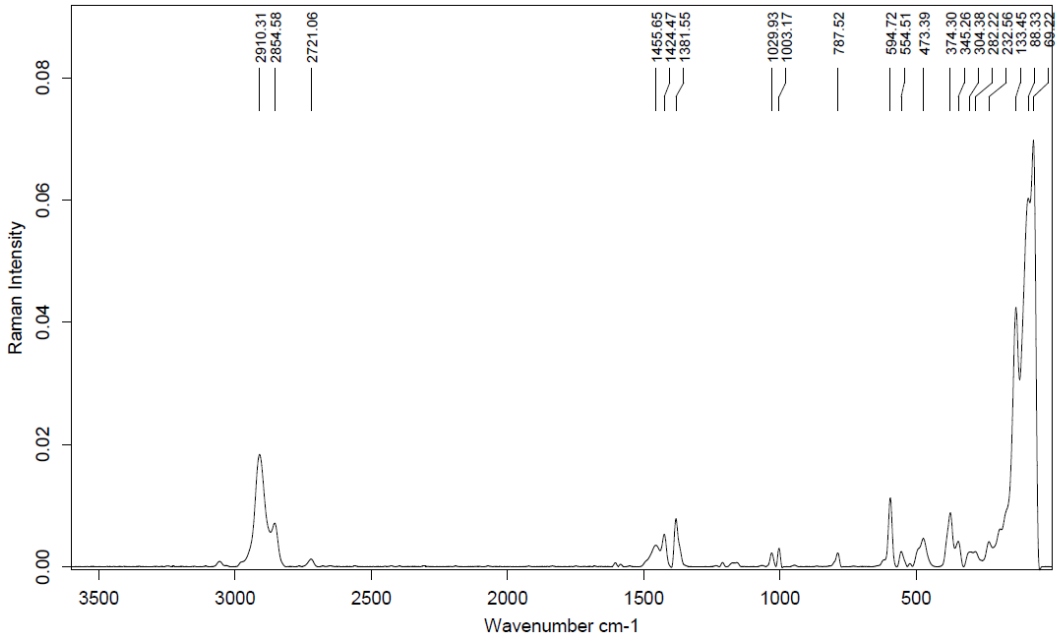

Figure S11: FT-Raman spectrum of $[(Cp^*Al)_6As_5Al]$ (**2**).

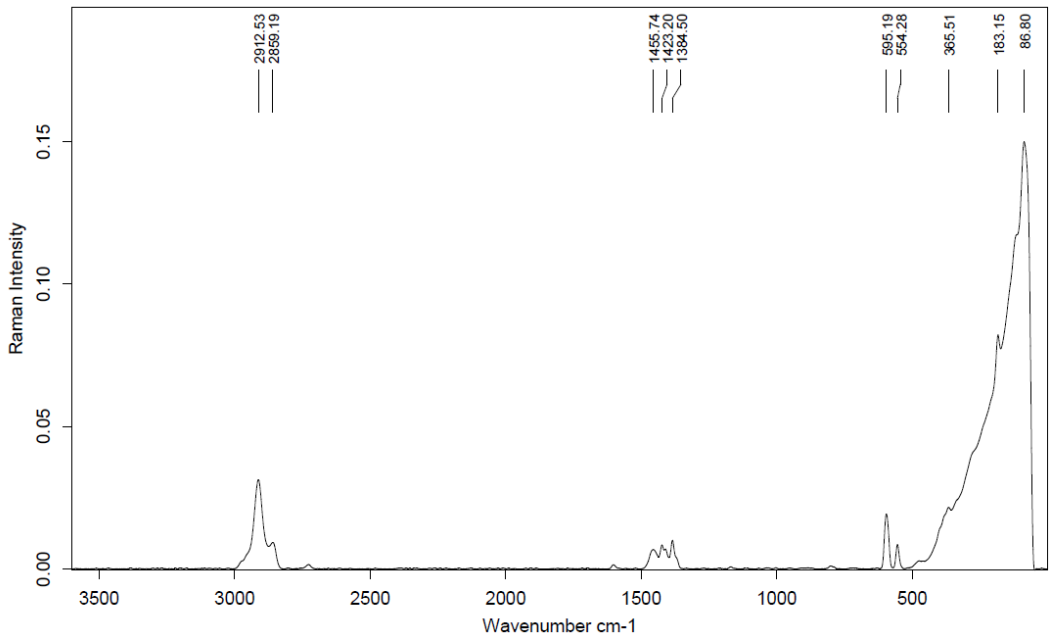

Figure S12: FT-Raman spectrum of $[(Cp^*AlBr)_3As]$ (**4**).

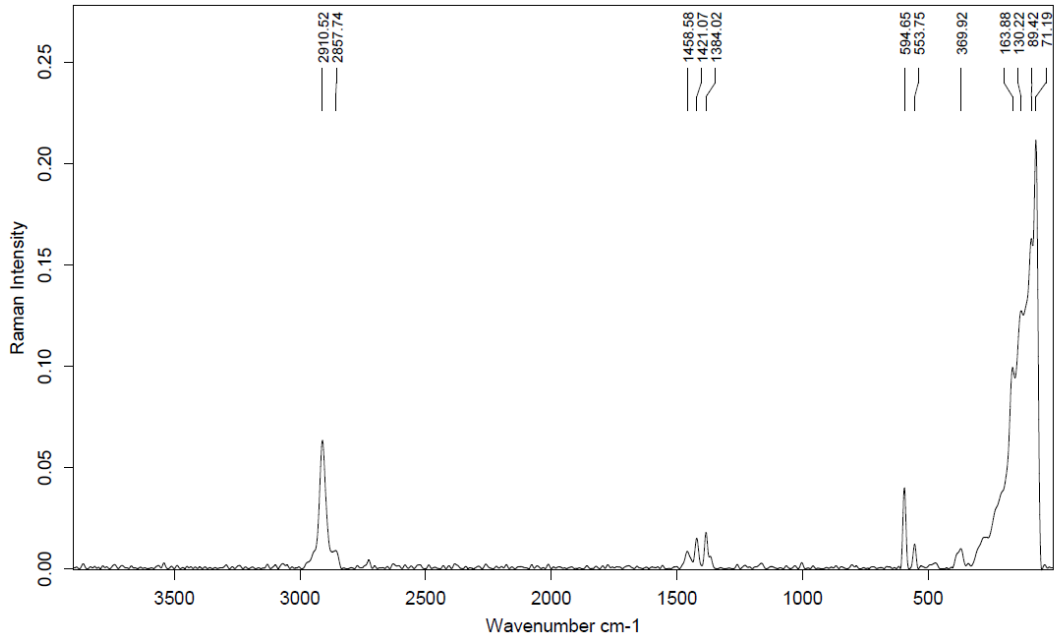

Figure S13: FT-Raman spectrum of $[(Cp^*All)_3As]$ (**5**).

X-ray Crystallographic Studies

Suitable crystals were selected under an optic microscope equipped with polarizing filters, covered in mineral oil (Aldrich) and mounted on a MiTeGen holder. Subsequently, the crystals were directly transferred to the cold stream of a STOE IPDS 2 (150 K) or STOE StadiVari (100 K) diffractometer, equipped with a Mo-sealed tube or a MoGenix 3D HF x-ray source, respectively. All structures were solved using the programs SHELXS/T and Olex2 1.3.[8, 9, 10] The remaining non-hydrogen atoms were located from successive difference Fourier map calculations. The refinements were carried out by using full-matrix least-squares techniques on F^2 by using the program SHELXL. In each case, the locations of the largest peaks in the final difference Fourier map calculations, as well as the magnitude of the residual electron densities, were of no chemical significance. Specific comments on the structures discussed here are given below.

$[(Cp^*Al)_6As_4]$ (**1**): The asymmetric unit of compound **1** contains two molecules of toluene with a chemical occupancy of 25%. One could be modelled using SIMU restraints and negative PART instructions (see Fig. S15 for comparison of modelled toluene moiety and symmetry generated disordered toluene moiety in the unit cell). The other could not be modelled satisfactorily. Therefore, the correlated electron density from the second toluene moiety was removed from the electron density map using the solvent mask algorithm of Olex2.[10]

$[(Cp^*Al)_6As_5Al]$ (**2**): The asymmetric unit of compound **2** contains two molecules of benzene. One with a chemical occupancy of 100% and another molecule with a chemical occupancy of 25% on a special position. The latter was modelled using negative PART instructions and SIMU restraints (see Fig. S17 for comparison of modelled benzene moiety and symmetry generated disordered benzene moiety in the unit cell).

$[(Cp^*Al)_3Sb]$ (**3**): Structure known from literature.[6, 7] Cell found by SCXRD:

a = b = 11.120(2) Å	α = β = 90°	V = 1579.9(6) Å^3
c = 14.753(4) Å	γ = 120°	

$[(Cp^*AlI)_3As]$ (**5**): Compound **5** showed indications of inversion twinning. Therefore, the twin command of SHELXL was applied using the appropriate twin law for an inversion twin [-1, 0, 0, 0, -1, 0, 0, 0, -1] and a BASF [0.441]. This resulted in significantly better R values.

Crystallographic data for the structures reported in this paper have been deposited with the Cambridge Crystallographic Data Centre as a supplementary publication no. 2071388-2071391. Copies of the data can be obtained free of charge on application to CCDC, 12 Union Road, Cambridge CB21EZ, UK (fax: (+(44)1223-336-033; email: deposit@ccdc.cam.ac.uk).

Table S1: Crystal data and structure refinement of 1, 2, 4 and 5.

Compound	**1**	**2**	**4**	**5**
Formula	$C_{74}H_{106}Al_6As_4$	$C_{72}H_{102}Al_7As_5$	$C_{30}H_{45}Al_3AsBr_3$	$C_{30}H_{45}Al_3AsI_3$
$D_{calc.}$/ g cm^{-3}	1.339	1.397	1.602	1.825
μ/mm^{-1}	1.946	2.396	4.729	3.787
Formula Weight	1457.14	1530.99	801.25	942.22
Color	clear yellow	clear dark red	clear yellow	clear yellow
Shape	rod	fragment	irregular	rod
Size/mm^3	0.28×0.14×0.05	0.24×0.12×0.05	0.34×0.25×0.17	0.32×0.20×0.13
T/K	100	100	100	150
Crystal System	monoclinic	orthorhombic	triclinic	trigonal
Space Group	*C2/m*	*Pnma*	*P*-1	*R*3
a/Å	21.9888(9)	31.0554(10)	11.3402(4)	18.8356(10)
b/Å	17.1848(6)	17.2141(4)	16.7244(7)	-
c/Å	10.7513(4)	13.6117(3)	18.6143(8)	8.3718(6)
α/°	-	-	95.614(3)	-
β/°	117.164(3)	-	90.722(3)	-
γ/°	-	-	108.785(3)	-
V/Å^3	3614.5(3)	7276.7(3)	3322.6(2)	2572.2(3)
Z	2	4	4	3
Z'	0.25	0.5	2	0.333333
Wavelength/Å	0.71073	0.71073	0.71073	0.71073
Radiation type	Mo K$_a$	Mo K$_a$	Mo K$_a$	Mo K$_a$
Q_{min}/°	1.577	2.315	1.606	2.162
Q_{max}/°	31.620	29.474	31.365	29.431
Measured Refl.	17651	23729	32558	8313
Independent Refl.	5274	9378	17117	3183
Reflections with I > 2(I)	4228	7207	12003	3009
R_{int}	0.0324	0.0214	0.0419	0.0205
Parameters	225	476	697	117
Restraints	36	72	0	1
Largest Peak	0.796	0.432	0.744	0.374
Deepest Hole	-0.400	-0.448	-0.686	-0.429
GooF	1.024	1.023	1.015	1.083
wR_2 (all data)	0.1063	0.0722	0.1291	0.0601
wR_2	0.0988	0.0652	0.1123	0.0597
R_1 (all data)	0.0524	0.0556	0.0791	0.0273
R_1	0.0386	0.0337	0.0476	0.0253
Flack Parameter	-	-	-	0.432(9)

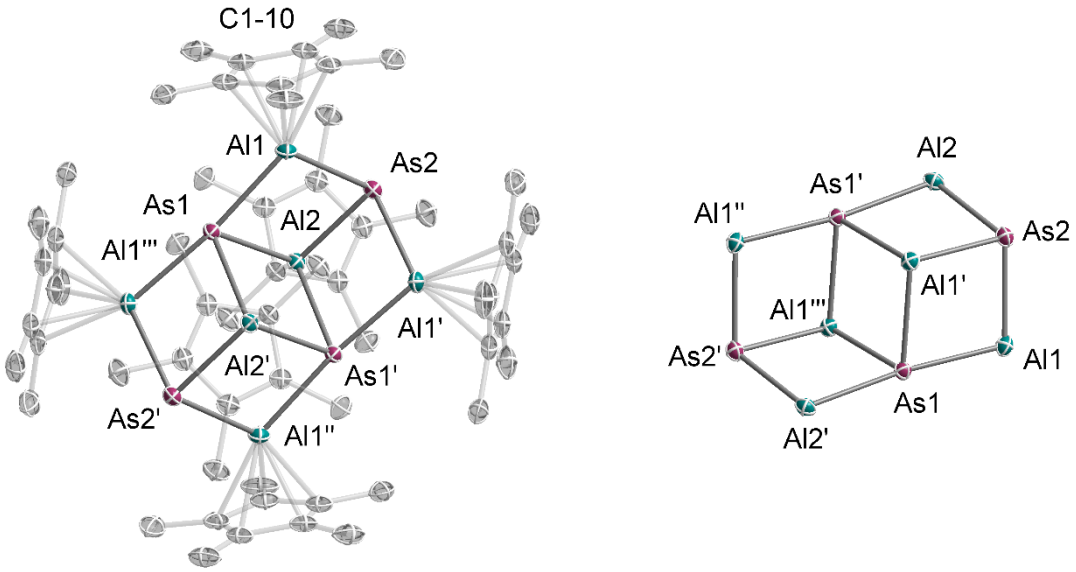

Figure S14: Left: Molecular structure of **1** in the solid state. Thermal ellipsoids are represented at 50% probability. Cp*-ligands are transparent, hydrogen atoms and two molecules of toluene are omitted for clarity. For selected bond lengths and angles see table S2. Right: core structure of compound **1** without Cp*-ligands. Colour code: As (dark red), Al (light blue), C (transparent black).

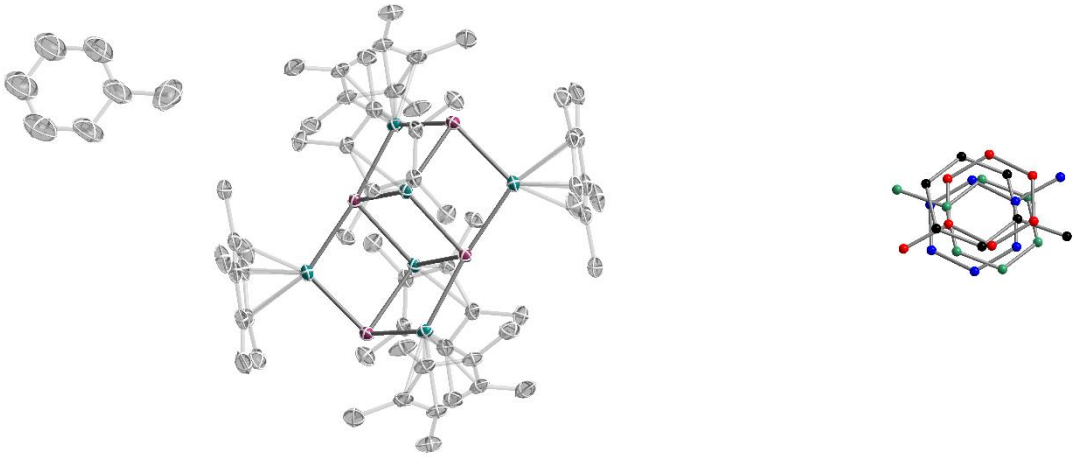

Figure S15: Left: Molecular structure of **1** in the solid state with modelled toluene molecule on special position. Right: Symmetry generated disordered toluene moiety in the unit cell.

Table S2: Selected bond lengths and angles for [(Cp*Al)$_6$As$_4$] (**1**); Ct_{Cp^*} = Centroid of the Cp*-ring moiety.

Length/ Å			**Angle/°**			
As1	Al2	2.5019(6)	Al1	As1	Al2	78.20(2)
As1	Al1	2.4730(7)	Al1	As2	Al2	80.01(2)
As2	Al2	2.4619(9)	As2	Al2	As1	99.23(2)
As2	Al1	2.4186(7)	As2	Al1	As1	101.23(2)
Al2	C11	2.067(3)				
Al1	C4	2.238(2)				
Al1	C2	2.290(2)				
Al1	C3	2.226(2)				
Al1	C5	2.238(2)				
Al1	Ct_{Cp^*}	1.9066(8)				
Al2	Ct_{Cp^*}	2.564(2)				

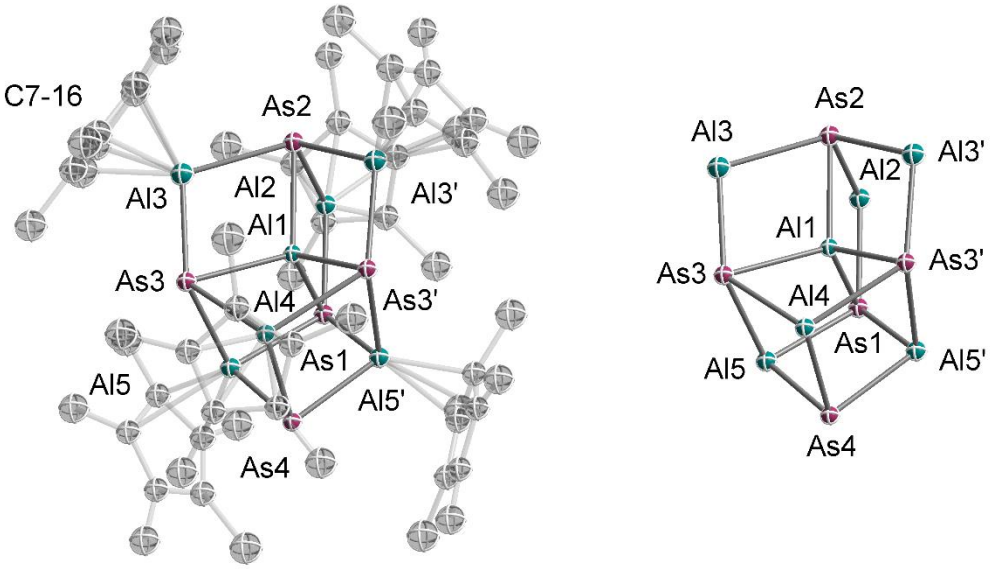

Figure S16: Left: Molecular structure of **2** in the solid state. Thermal ellipsoids are represented at 50% probability. Cp*-ligands are transparent, hydrogen atoms and two molecules of benzene are omitted for clarity. For selected bond lengths and angles see table S3. Right: core structure of compound **2** without Cp*-ligands. Colour code: As (dark red), Al (light blue), C (transparent black).

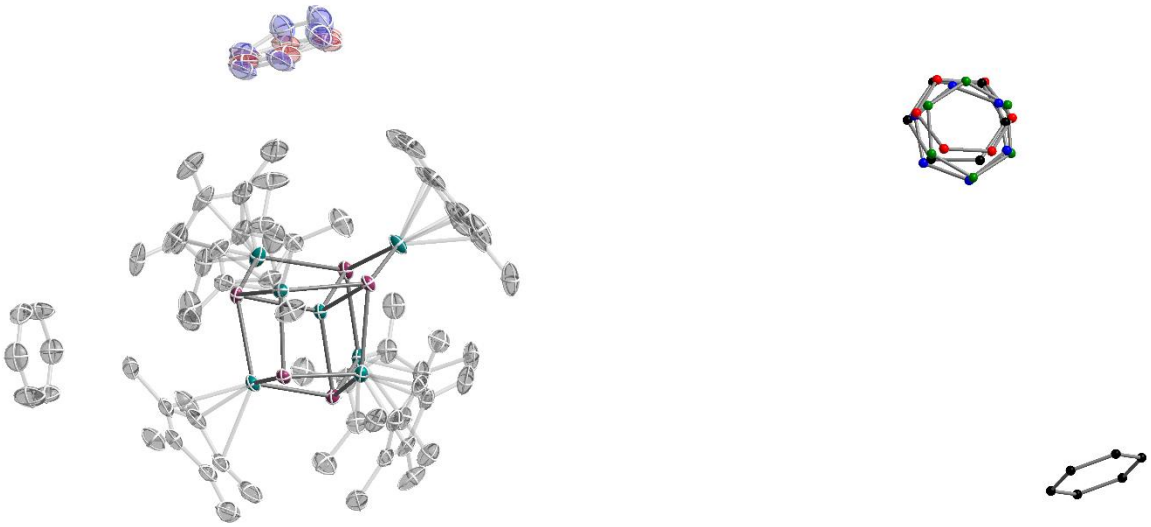

Figure S17: Left: Molecular structure of **2** in the solid state with modelled benzene molecules (top one on special position). Different parts of the disordered benzene are marked by blue and red colour. Right: Symmetry generated disordered benzene moiety in the unit cell.

Table S3: Selected bond lengths and angles for $[(Cp^*Al)_6As_5Al]$ (**2**); Ct_{Cp^*} = Centroid of the Cp*-ring moiety.

Length/ Å			Angle/°			
As1	Al1	2.4730(10)	As3	Al1	As3'	111.13(4)
As1	Al5	2.5759(8)	As3	Al1	As2	108.56(3)
As1	Al2	2.4302(11)	As2	Al1	As1	106.60(4)
As2	Al1	2.4718(10)	As2	Al1	As1	106.60(4)
As2	Al2	2.5455(12)				
As2	Al3	2.5621(8)				
As3	Al1	2.4493(6)				
As3	Al5	2.5757(8)				
As3	Al4	2.6264(7)				
As3	Al3	2.4091(8)				
As4	Al5	2.4424(7)				
As4	Al4	2.4609(11)				
Al2	Ct_{Cp^*}	1.896(2)				
Al3	Ct_{Cp^*}	1.904(2)				
Al4	Ct_{Cp^*}	2.092(2)				
Al5	Ct_{Cp^*}	2.360(2)				

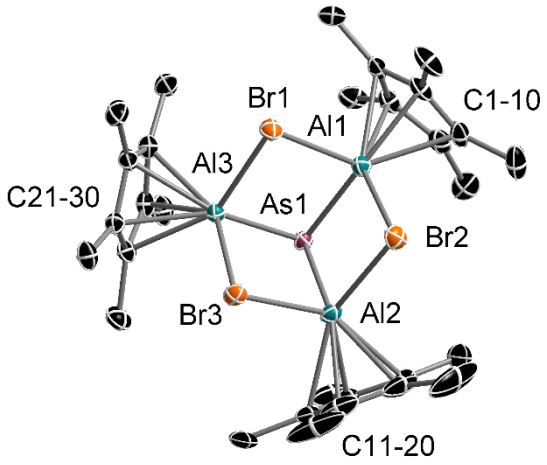

Figure S18: Molecular structure of **4** in the solid state. Thermal ellipsoids are represented at 50% probability. Hydrogen atoms are omitted for clarity. For selected bond lengths and angles see table S4. Colour code: As (dark red), Al (light blue), C (black), Br (orange).

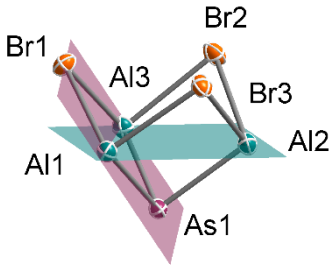

Figure S19: Side view of the *calix*-like core structure of **4**. Al1-Al2-Al3 plane (light blue) and As1-Al1-Al3-Br1 plane (dark red) are illustrated for clarification of the opening angle. Colour code: As (dark red), Al (light blue), Br (orange).

Table S4: Selected bond lengths and angles for $[(Cp^*AlBr)_3As]$ (**4**); Ct_{Cp^*} = Centroid of the Cp*-ring moiety.

Length/ Å			**Angle/°**			
As1	Al3	2.4374(12)	Al2	As1	Al3	86.93(4)
As1	Al2	2.4236(13)	Al1	As1	Al3	86.21(4)
As1	Al1	2.4118(13)	Al1	As1	Al2	85.84(4)
Br1	Al3	2.5611(12)	Al3	Br1	Al1	80.25(4)
Br1	Al1	2.5806(13)	Al3	Br3	Al2	81.01(4)
Al1	Ct_{Cp^*}	1.9647(12)	Al1	Br2	Al2	79.19(4)
Al2	Ct_{Cp^*}	1.9260(14)	*calix* opening angle			124.12
Al3	Ct_{Cp^*}	1.9194(12)				

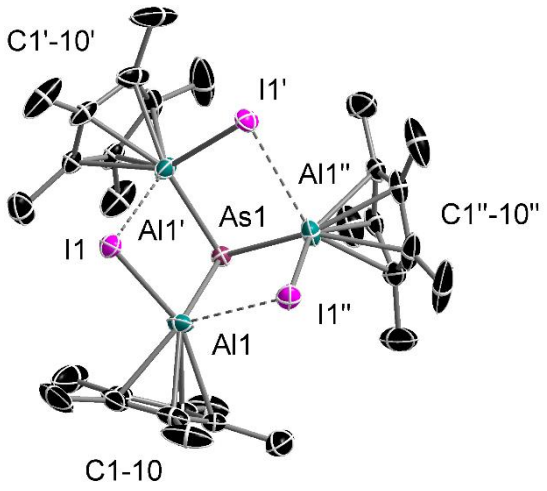

Figure S20: Molecular structure of **5** in the solid state. Thermal ellipsoids are represented at 50% probability. Hydrogen atoms are omitted for clarity. For selected bond lengths and angles see table S5. Colour code: As (dark red), Al (light blue), C (black), I (purple).

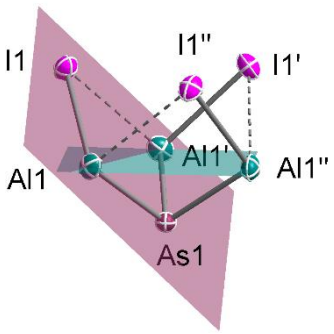

Figure S21: Side view of the c*alix*-like core structure of **5**. Al1-Al1'-Al1'' plane (light blue) and As1-Al1-Al1'-I1 plane (dark red) are illustrated for clarification of the opening angle. Colour code: As (dark red), Al (light blue), I (purple).

Table S5: Selected bond lengths and angles for [(Cp*AlI)$_3$As] (**5**); Ct_{Cp^*} = Centroid of the Cp*-ring moiety. I1-Al1' distance listed for comparison with I1-Al1 bond length.

Length/ Å			**Angle/°**			
I1	Al1	2.706(2)	As1	Al1	I1	102.32(6)
As1	Al1	2.407(2)	Al1'	As1	Al1	92.21(6)
Al1	Ct_{Cp^*}	1.946(2)	*calix* opening angle			125.59
I1	Al1'	3.088(2)				

References

1. C. Schoo, S. Bestgen, A. Egeberg, S. Klementyeva, C. Feldmann, S. N. Konchenko and P. W. Roesky, *Angew. Chem. Int. Ed.*, 2018, **57**, 5912-5916.
2. C. Schoo, S. Bestgen, A. Egeberg, J. Seibert, S. N. Konchenko, C. Feldmann and P. W. Roesky, *Angew. Chem. Int. Ed.*, 2019, **58**, 4386-4389.
3. M. Schormann, K. S. Klimek, H. Hatop, S. P. Varkey, H. W. Roesky, C. Lehmann, C. Röpken, R. Herbst-Irmer and M. Noltemeyer, *J. Solid State Chem.*, 2001, **162**, 225-236.
4. A. Hofmann, A. Lamprecht, O. F. González-Belman, R. D. Dewhurst, J. O. C. Jiménez-Halla, S. Kachel and H. Braunschweig, *Chem. Commun.*, 2018, **54**, 1639-1642.
5. S. G. Minasian and J. Arnold, *Chem. Commun.*, 2008, DOI: 10.1039/B806804F, 4043-4045.
6. S. Schulz, T. Schoop, H. W. Roesky, L. Häming, A. Steiner and R. Herbst-Irmer, *Angew. Chem. Int. Ed.*, 1995, **34**, 919-920.
7. C. Ganesamoorthy, J. Krüger, E. Glöckler, C. Helling, L. John, W. Frank, C. Wölper and S. Schulz, *Inorg. Chem.*, 2018, **57**, 9495-9503.
8. G. Sheldrick, *Acta Cryst. A*, 2015, **71**, 3-8.
9. G. Sheldrick, *Acta Cryst. C*, 2015, **71**, 3-8.
10. O. V. Dolomanov, L. J. Bourhis, R. J. Gildea, J. A. K. Howard and H. Puschmann, *J. Appl. Crystallogr.*, 2009, **42**, 339-341.